J Supercond Nov Magn (2012) 25:1159–1167
DOI 10.1007/s10948-011-1383-2

ORIGINAL PAPER

# Entanglement Study of the 1D Ising Model with Added Dzyaloshinskii–Moriya Interaction

**J. Vahedi · M.R. Soltani · S. Mahdavifar**

Received: 31 October 2011 / Accepted: 30 November 2011 / Published online: 22 December 2011


**Abstract** We have studied occurrence of quantum phase transition in the one-dimensional spin-1/2 Ising model with added Dzyaloshinskii–Moriya (DM) interaction from a bipartite and multipartite entanglement point of view. Using exact numerical solutions, we are able to study such systems up to 24 qubits. The minimum of the entanglement ratio $R \equiv \tau_2/\tau_1 < 1$, as a novel estimator of QPT, has been used to detect QPT and our calculations have shown that its minimum took place at the critical point. We have also shown both the global-entanglement (GE) and multipartite entanglement (ME) are maximal at the critical point for the Ising chain with added DM interaction. Using the matrix product state approach, we have calculated the tangle and concurrence of the model and it is able to capture and confirm our numerical experiment result. Lack of inversion symmetry in the presence of DM interaction stimulated us to study entanglement of three qubits in a symmetric and nonsymmetric way.

**Keywords** Entanglement · Ising chain · Dzyaloshinsky–Moriya interaction

## 1 Introduction

In the last few years, it has become apparent that quantum information may lead to further insight into other areas of physics such as condensed matter and statistical mechanics [1–12]. The attention of the quantum information community to study in condensed matter has stimulated an exciting cross fertilization between the two areas. It has been found that entanglement plays a crucial role in the low-temperature physics of many of these systems, particularly in their ground state [4–7, 10]. Quantum phase transition (QPT) happens at zero temperature and shows nonanalyticity in the physical properties of the ground state by the change of a parameter $\lambda$ of the Hamiltonian $H(\lambda)$. This change is driven only by quantum fluctuations [13]. Since QPT occurs at $T = 0$, the emerging correlations have a purely quantum origin. Therefore, it is reasonable to conjecture that entanglement is a crucial ingredient for the occurrence of the QPT [4, 6, 7, 14–16]. Wu et al. [7] have shown that a discontinuity in a bipartite entanglement measure (concurrence [15] and negativity [16]) is a necessary and sufficient indicator of a first-order quantum phase transition; negativity being characterized by a discontinuity in the first derivative of the ground state energy. They have also shown that a discontinuity or a divergence in the first derivative of the same measure (assuming it is continuous) is a necessary and sufficient indicator of a second-order QPT that is characterized by a discontinuity or a divergence of the second derivative of the ground state energy.

Dzyaloshinskii has shown [17] that, in crystal with no inversion center, the usual isotropic exchange $J\vec{S}_i.\vec{S}_j$ is not the only magnetic interaction and antisymmetric exchange $\vec{D}_{ij}.(\vec{S}_i \times \vec{S}_j)$ is allowed. Later, Moriya has shown [18] that inclusion of spin orbit coupling on magnetic ions in 1st and 2nd order leads to antisymmetric and anisotropic exchange, respectively. This interaction is, however, rather difficult to handle analytically [19, 20], but it is one of the agents responsible for magnetic frustration. Since this interaction may induce spiral spin arrangements in the ground

J. Vahedi (✉) · M.R. Soltani
Department of Physics, Science and Research Branch, Islamic Azad University, Tehran, Iran
e-mail: javahedi@iausari.ac.ir

S. Mahdavifar
Department of Physics, University of Guilan, 41335-1914, Rasht, Iran

state [21], it is closely involved with ferroelectricity in multiferroic spin chains [22, 23]. Besides, the DM interaction plays an important role in explaining the electron spin resonance experiments in some one-dimensional antiferromagnets [24, 25]. Moreover, the DM interaction modifies the dynamic properties [26] and quantum entanglement [27] of spin chains [28]. In the present paper, we are interested to study the one-dimensional spin-1/2 Ising model with added DM interaction from the quantum entanglement point of view using variational matrix product state and numerical exact diagonalization methods. The Hamiltonian is given by

$$H = J\sum_{j=1}^{N} S_j^z S_{j+1}^z + \sum_{j=1}^{N} \vec{D}.\big(\vec{S}_j \times \vec{S}_{j+1}\big), \tag{1}$$

where $\overrightarrow{S}_j$ is spin-1/2 operator on the $j$th site, and $J > 0$ ($J < 0$) denotes antiferromagnetic (ferromagnetic) coupling constant. In the very recent works [29, 30], the authors have studied the ground state phase diagram of the ferromagnetic and antiferromagnetic Ising chain in the presence of the uniform DM interaction. It is found that the ground state phase diagram of both systems consists of spiral-ferromagnetic and spiral-antiferromagnetic phases, respectively, and a commensurate-incommensurate (C-IC) quantum phase transition occurs at $D_c = |J|$. However, at the critical value $D_c$, a metamagnetic phase transition occurs into the chiral gapless phase in the ground state phase diagram of the ferromagnetic chain.

This paper is structured as follows. In Sect. 2, we will discuss about bipartite and multipartite entanglement measures as QPT indicators of our model and we will present our numerical study. In Sect. 3, the variational matrix product states will be outlined and bipartite entanglement will be obtained. In Sect. 4, we will study entanglement of three qubits in the symmetric and antisymmetric way. Finally, we conclude and summarize our results in Sect. 5.

## 2 Quantum Phase Transition

### 2.1 Bipartite Entanglement

The occurrence of collective behavior in many-body quantum systems is associated with classical and quantum correlation. The quantum correlations, known as entanglement, cannot be measured in terms of classical physics and represents the impossibility of giving a local description of many-body quantum state. The issue of finding entanglement measures has recently attracted an increasing interest [5, 6, 31, 32]. Concurrence and tangle are among the most widely used measures in QPT related entanglement studies. Both of these measures are for bipartite states and because of the monogamous nature of entanglement they are expected to decrease at the quantum critical point, if entanglement is shared by the whole system.Therefore, in order to manifest the presence of (QPT) in the model described by (1), we focus on the entanglement of formation [33] in the quantum spin system and make use of the *one-tangle* and of the concurrence. The one-tangle [34, 35] quantifies the zero temperature entanglement of a single spin with the rest of the system and defines as

$$\tau_1 = 4\det\rho^{(1)}, \quad \rho^{(1)} = \frac{1}{2}\Big(I + \sum_{\alpha} M^{\alpha} S^{\alpha}\Big), \tag{2}$$

where $\rho^{(1)}$ is the one-site reduced density matrix, $M^{\alpha} = \langle S^{\alpha}\rangle$, and $\alpha = x, y, z$. In terms of the spin expectation values $M^{\alpha}$, one has

$$\tau_1 = 1 - 4\sum_{\alpha}\big(M^{\alpha}\big)^2. \tag{3}$$

On other hand, the concurrence [15] quantifies the pairwise entanglement between two spins and defines as

$$C_{lm} = 2\max\big\{0, C_{lm}^{(1)}, C_{lm}^{(2)}\big\}, \tag{4}$$

where

$$\begin{aligned} C_{lm}^{(1)} &= \sqrt{\big(g_{lm}^{xx} - g_{lm}^{yy}\big)^2 + \big(g_{lm}^{xy} + g_{lm}^{yx}\big)^2} \\ &\quad - \sqrt{\Big(\frac{1}{4} - g_{lm}^{zz}\Big)^2 - \Big(\frac{M_l^z - M_m^z}{2}\Big)^2}, \\ C_{lm}^{(2)} &= \sqrt{\big(g_{lm}^{xx} + g_{lm}^{yy}\big)^2 + \big(g_{lm}^{xy} - g_{lm}^{yx}\big)^2} \\ &\quad - \sqrt{\Big(\frac{1}{4} + g_{lm}^{zz}\Big)^2 - \Big(\frac{M_l^z + M_m^z}{2}\Big)^2} \end{aligned} \tag{5}$$

and $g_{lm}^{\alpha\beta} = \langle S_l^{\alpha} S_m^{\beta}\rangle$ is the correlation function between spins on sites $l$ and $m$ and $M_l^z = \langle S_l^z\rangle$. The notation $\langle\ldots\rangle$ represents the ground state expectation value. One-tangle and concurrence are related by Coffman–Kundu–Wootters (CKW) conjecture [35], which had been proved by Osborne and Verstraete [36], stating that

$$\tau_1 \geq \tau_2 \equiv \sum_{l\neq m} C_{lm}^2 \tag{6}$$

which expresses the crucial fact that pairwise entanglement does not exhaust the global entanglement of the system, as entanglement can also be stored in 3-spin correlations, 4-spin correlations, and so on. Authors in [28, 29] have proposed that, due to CKW conjecture, the minimum of the entanglement ratio $R \equiv \tau_2/\tau_1 < 1$, as a novel estimator of QPT, fully based on entanglement quantifiers.

By doing an experiment, one can find a clear picture of the entanglement phenomenon in the ground state magnetic phases of the model. Since a real experiment cannot be done at zero temperature, the best way is doing a virtual numerical experiment. A very famous and accurate method in the

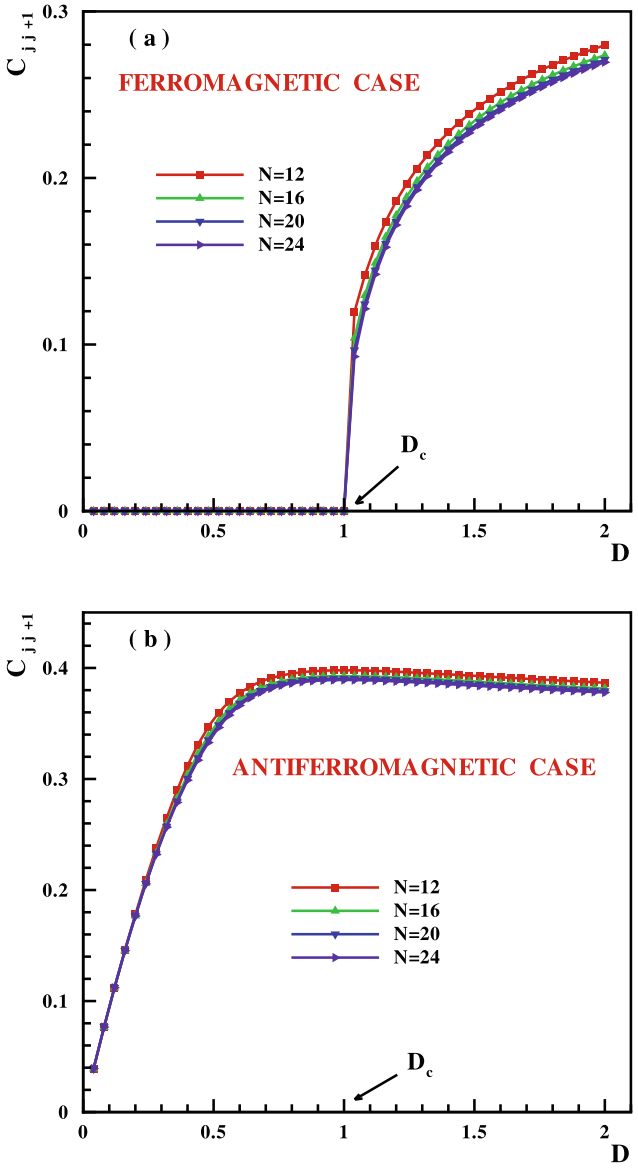


**Fig. 1** (Color online) The concurrence is plotted as a function of DM vector $D$, (**a**) ferromagnetic and (**b**) antiferromagnetic cases for different lengths $N = 12, 16, 20, 24$

field of the numerical experiments is known as the Lanczos method. However, the strong role of a numerical experiment to examine quantum phase transitions is not negligible. To explore the nature of the entanglement in different magnetic phases, we used Lanczos method to diagonalize numerically chains with length up to $N = 24$ and coupling constant $|J| = 1$. The ground state eigenvector, $|Gs\rangle$, was obtained for chains with periodic boundary condition. The numerical Lanczos results on the concurrence for the Ising chain with DM interaction, are shown in Fig. 1. As is clearly seen from Fig. 1(a), in the case of the ferromagnetic chain and for $D < D_c = |J| = 1$, the concurrence is equal to zero which shows that the ground state of the system is in the fully non-entangled polarized ferromagnetic phase. At the critical value $D_c = |J| = 1$, the concurrence jumps to a nonzero value which confirms the metamagnetic phase transition. By further increasing the DM vector, $D > D_c$, the ground state is in the chiral phase and nearest neighbors are entangled. On the other hand, in the case of the antiferromagnetic Ising model, as can be clearly seen from Fig. 1(b), in the absence of the DM interaction, the ground state is nonentangled which is related to the saturated Néel phase. As soon as the DM vector applies, nearest neighbors will be entangled and concurrence between them increases from zero. Thus, in the case of antiferromagnetic Ising chains, the DM interaction induces the quantum correlations of the two spins and nearest neighbor spins will be entangled as soon as the DM interaction applies. In contrast, in the case of the ferromagnetic Ising chains, the DM interaction only induces the quantum correlations after the critical value $D_c$ and nearest neighbor spins will not be entangled up to the critical value $D_c$.

An additional insight into the nature of different phases can be obtained by studying the entanglement ratio. Therefore, we have calculated the entanglement ratio by using the Lanczos method in both ferromagnetic and antiferromagnetic cases. We have plotted our numerical results in Fig. 2. For the ferromagnetic case, as it can be seen from Fig. 2(a), the entanglement ratio remains zero up to the critical DM interaction $D_c$ which is expected from the saturated ferromagnetic phase. As soon as the DM interaction increases from the critical $D_c$, the entanglement ratio starts to increase from zero. In the inset of Fig. 2(a), the first derivative entanglement ratio is plotted. As it is seen in the ferromagnetic phase, $D < D_c$, the derivative is equal to zero and an abrupt change took place exactly at $D_c = |J| = 1$ which is an indication of the quantum phase transition. In the antiferromagnetic case, Fig. 2(b), as soon as the DM interaction applies the entanglement ratio creates and decreases by increasing the DM vector up to $D_c = 1.0$ which a change took place and in the $D > D_c$ region the ratio becomes monotonous. In the inset of Fig. 2(b), the first derivative entanglement ratio is plotted. It is clear that in the $D > D_c$ region derivative of ratio is equal to zero and an abrupt change took place exactly at $D_c = |J| = 1.0$ which is an indication of the quantum phase transition. The oscillations of ratio at finite N in the region $D < D_c$ is the result of level crossing between the ground state and excited states of the model.

## 2.2 Global Entanglement

Because of many different kinds of entanglement, quantifying of multipartite entanglement states (MES) is more difficult. Global-entanglement ($E_{gl}$) measure defined by Meyer

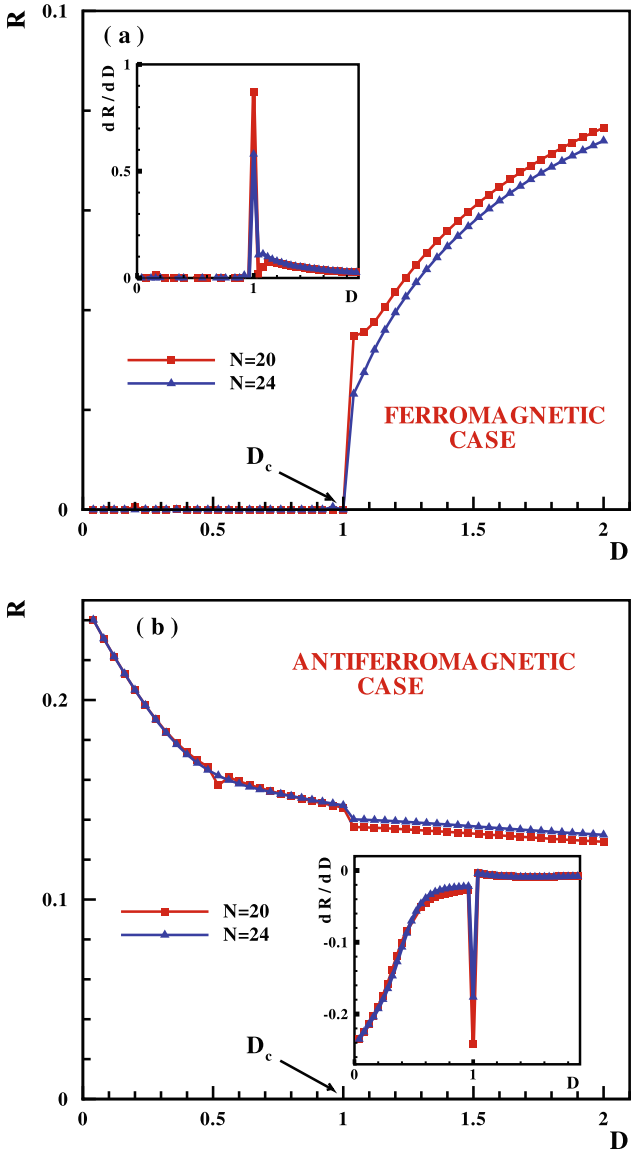


**Fig. 2** (Color online) The entanglement ratio $\tau_1/\tau_2 = R$ is plotted as a function of DM vector $D$, (**a**) ferromagnetic and (**b**) antiferromagnetic cases for different lengths $N = 20, 24$. *Inset*: the first derivative of entanglement ratio

and Wallach [37] which can measure the total nonlocal information per particle in a general multipartite system [38]

$$E_{\mathrm{gl}} = \frac{1}{N}\left[2\sum_{i_1<i_2}\tau_{i_1 i_2} + \cdots + N\sum_{i_1<\cdots<i_N}\tau_{i_1\cdots i_N}\right]. \tag{7}$$

$E_{\mathrm{gl}}$ is the average of tangles per particles ($\frac{\langle\tau\rangle}{N}$), without giving detailed knowledge of tangle distribution among the individual particles. Therefore, $E_{\mathrm{gl}}$ is an average quantity and cannot distinguish between entangled states which have equal $\langle\tau\rangle$ yet different distributions of tangles, like $\mathrm{GHZ}_N$ (Greenberger–Horne–Zeilinger) and $\mathrm{EPR}^{\otimes N/2}$ state. $E_{\mathrm{gl}}$ has ability to discriminate between GHZ from $W$ states because of their different values of tangle. De Oliveira et al. [39–41] also introduced a slight extension of global entanglement as generalized global entanglement (GGE) which, in contrast to global entanglement, can distinguish the three paradigmatic entangled $\mathrm{GHZ}_N$ (Greenberger–Horne–Zeilinger), $\mathrm{EPR}^{\otimes N/2}$ and W states.

$$G(2,n) = \frac{4}{3}\frac{1}{N-1}\sum_{n=1}^{N-1}\left[1 - \frac{1}{N-1}\sum_{j}^{N} Tr\rho_{j,j+n}^2\right], \tag{8}$$

where $\rho_{j,j+n}$ is the reduced density matrix obtained by tracing away from the ground state all spins except the $(j)$th and $(j+n)$th spins. As such the generalized measure can detect a genuine multipartite entanglement and is maximal at the critical point [39–41]. Here, we have calculated multipartite entanglement (8) by using Lanczos numerical method with periodic boundary condition in antiferromagnetic case. We have plotted our numerical results in Fig. 3 for the antiferromagnetic case. As it can be seen from Fig. 3(a) the multipartite entanglement starts to increase by increasing DM up to the critical DM interaction $D_{\mathrm{c}}$ where a change took place exactly at $D_{\mathrm{c}} = |J| = 1$ and then after that the multipartite entanglement reaches the saturation value. Our calculation shows that multipartite entanglement is maximal around the critical point $D_{\mathrm{c}}$. In order to get better insight into the ability of multipartite entanglement as a quantum phase transition toolkit, we have plotted the first derivative entanglement multipartite entanglement in the inset of Fig. 3(a). It shows divergent behavior at the critical point $D_{\mathrm{c}}$. We have also plotted $\lim_{n\to\infty} G(2,n)$ in Fig. 3(b). Our calculation shows $G(2,n)$ increases as $n \to \infty$ at the critical point. To conclude, we have calculated global entanglement $E_{\mathrm{gl}}$ of model (1) and compare it with multipartite entanglement. It can be seen from Fig. 4 that both $G(2,1)$ and $E_{\mathrm{gl}}$ are maximal at the critical point $D_{\mathrm{c}}$ and their behavior is qualitatively the same.

## 3 Variational Matrix Product State Approach

The matrix product state is defined as [42–45]

$$|\psi\rangle = Tr(g_1, g_2, \ldots, g_N), \tag{9}$$

where $g_j = a_j|\uparrow\rangle_j + b_j|\downarrow\rangle_j$, and $a_j$ and $b_j$ are probability amplitudes for two spin configurations at site $j$. In what follows, we intend to determine the ground state energy of ferromagnetic Ising spin system with DM interaction. In this respect, by using the above formalism, the variational energy is obtained by

$$E_{\mathrm{var}} = \langle H\rangle = \frac{\langle\psi|H|\psi\rangle}{\langle\psi|\psi\rangle} = \sum_j \frac{\hat{H}_{j,j+1}}{[G_j, G_{j+1}]}, \tag{10}$$

where $\langle\psi|\psi\rangle = g_1\otimes g_1\otimes\cdots\otimes g_N\otimes g_N = \Pi_j G_j$ and $G_j = g_j\otimes g_j = |a_j|^2 + |b_j|^2$ here $\hat{H}_{jk} = J\hat{S}_j^z\hat{S}_k^z + \vec{D}.(\vec{S}_j\times\vec{S}_k)$

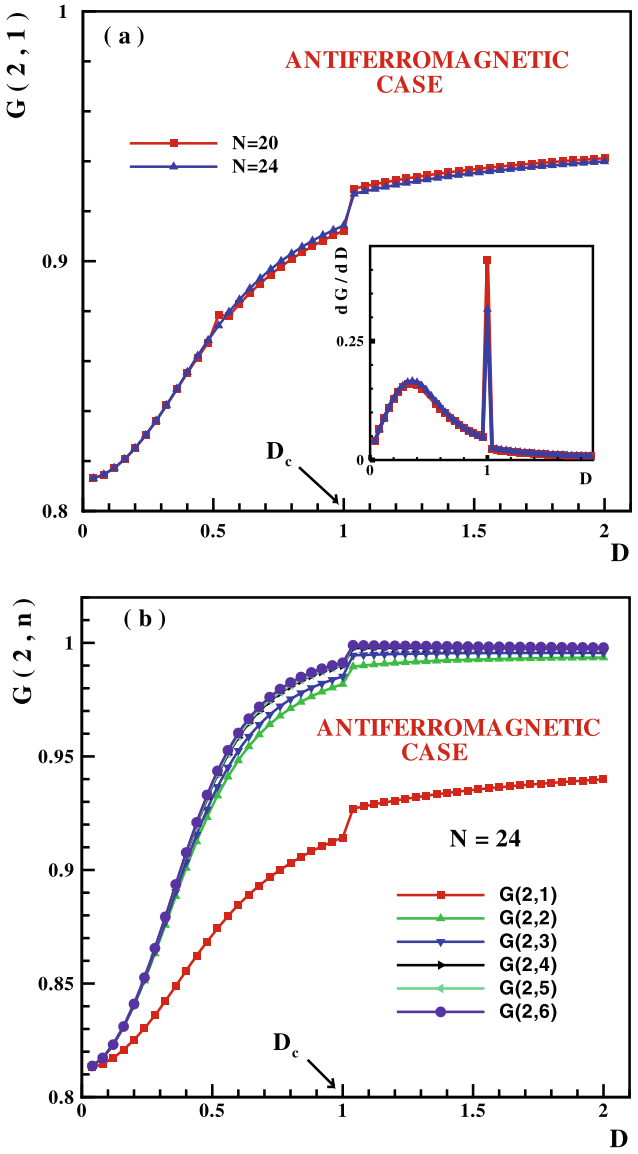


**Fig. 3** (Color online) (**a**) Multipartite entanglement estimator $G(2,1)$ is plotted as a function of DM vector $D$ for antiferromagnetic Ising chain with length $N = 20, 24$. *Inset*: the first derivative of multipartite entanglement $\frac{dG(2,n)}{dD}$. (**b**) $G(2,n)$ for the chain size $N = 24$, is plotted for several increasing values of $n$

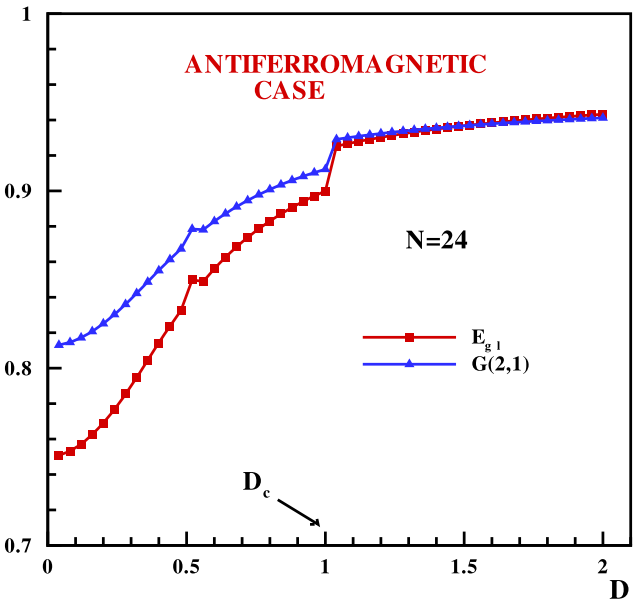


**Fig. 4** (Color online) Multipartite entanglement $G(2,n)$ and global entanglement $E_{\mathrm{gl}}$ are plotted as a function of DM vector $D$, for antiferromagnetic Ising chain with length $N = 24$

and $\hat{S}_j^{\alpha} = g_j \otimes \vec{S}_j^{\alpha} g_j$. The minimum of the variational energy function corresponds to the ground state energy of the system. Using the normalization condition $\langle\psi|\psi\rangle = 1$, we can map the variational parameter to $a_j = \cos(\theta_j)e^{i\varphi_j}$, $b_j = \sin(\theta_j)e^{\acute{\varphi_j}}$. Therefore, one can obtain $\hat{S}_j^z = \frac{1}{2}\cos(2\theta_j)$, $\hat{S}_j^+ = (\hat{S}_j^-)^\dagger = \frac{1}{2}\sin(2\theta_j)e^{i\phi_j}$ where $\phi_j = \varphi_j - \acute{\varphi_j}$ and by choosing $\vec{D} = D\hat{z}$, it is found that

$$E_{\mathrm{var}} = \frac{1}{4}\sum_j \big\{ J\cos(2\theta_j)\cos(2\theta_{j+1}) + D\sin(2\theta_j)\sin(2\theta_j)\sin(\phi_j - \phi_{j+1}) \big\}. \tag{11}$$

By minimizing the above equation, the ground state energy ($E_{\mathrm{GS}}$) in the ferromagnetic case $J < 0$ shall be obtained. It was shown in [26] that the ground state energy is the constant value, $E_{\mathrm{GS}} = -\frac{N|J|}{4}$ for $D < |J|$ and decreasing linearly with DM interaction for $D > |J|$ as $E_{\mathrm{GS}} = -\frac{ND}{4}$. Now, by using the minimized variational parameters of $E_{\mathrm{var}}$ we are able to calculate tangle (3) and concurrence (5). For $J > D$, one can obtain

$$\begin{aligned} &g_{j,j+1}^{xx} = g_{j,j+1}^{zz} = g_{j,j+1}^{yx} = g_{j,j+1}^{xy} = 0 \\ &g_{j,j+1}^{yy} = -1/4, \end{aligned} \tag{12}$$

and $M^z = 0$, so we have $\tau_1 = 1$ and $C_{j,j+1} = 1/2$. For $J < D$ again using the above conditions, one can obtain

$$\begin{aligned} &g_{j,j+1}^{xx} = g_{j,j+1}^{yy} = g_{j,j+1}^{yx} = g_{j,j+1}^{xy} = 0 \\ &g_{j,j+1}^{zz} = 1/4, \end{aligned} \tag{13}$$

and $M^z = 1/2$ which give $\tau_1 = 0$ and $C_{j,j+1} = 0$.

Figure 5 shows the ground state energy of the ferromagnetic Ising chain with DM interaction using variational matrix product state.

## 4 Three-Qubit Entanglement

In this section, lack of inversion symmetry in the presence of DM interaction stimulated us to study entanglement of formation of three-qubit in two inequivalent, symmetric, and nonsymmetric pairwise entanglement ways. By labeling the 3-qubits as 1, 2, 3 sequentially. The symmetric reduced density matrix $\rho_{13}$ is defined as $\rho_{13} = tr_2(\rho)$, where $\rho$ is the

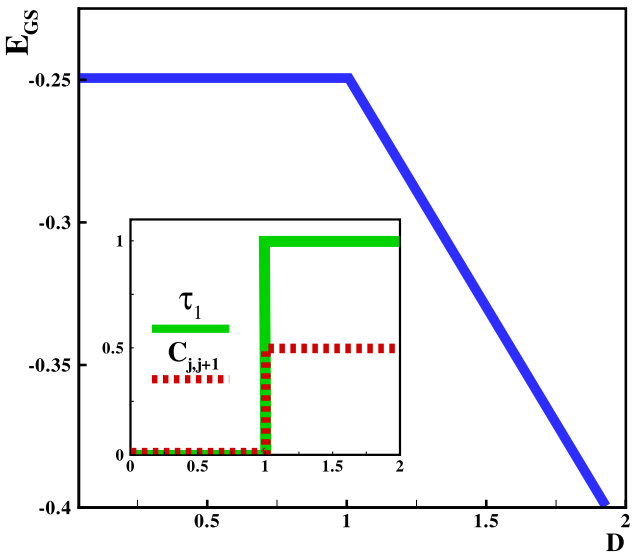


**Fig. 5** (Color online) The ground state energy (normalized by $N$) of ferromagnetic Ising chain with DM interaction using variational matrix product state. *Inset* shows one-tangle and concurrence as function of the DM interaction using variational matrix product state

density matrix of 3-qubits. The nonsymmetric reduced matrix is $\rho_{12} = tr_3(\rho)$. Before present our results, we briefly review the definition of concurrence [15, 35]. Let $\rho_{ij}$ be the density matrix of a pair of qubit $i$ and $j$. The concurrence corresponding to density matrix is defined as

$$C_{ij} = \max\{\lambda_1 - \lambda_2 - \lambda_3 - \lambda_4, 0\}, \tag{14}$$

where the quantities $\lambda_1 \geq \lambda_2 \geq \lambda_3 \geq \lambda_4$ are square roots of the eigenvalue of the operator

$$\varrho_{ij} = \rho_{ij}(\sigma_y \otimes \sigma_y)\rho_{ij}^*(\sigma_y \otimes \sigma_y). \tag{15}$$

The concurrence $C_{ij} = 0$ corresponds to an non-entangled state and $C_{ij} = 1$ corresponds to a maximally entanglement sate. A straightforward calculation gives the eigenstates and the eigenvalues of 3-qubit of (1). The square roots of the operator $\varrho_{ij}$ for symmetric and nonsymmetric cases are presented in sequence. In the symmetric case $\varrho_{13}$,

$$\lambda_1 = 4\left(\frac{2}{\alpha^2+2}\right)^2, \quad \lambda_2 = \lambda_3 = \left(\frac{\alpha^2}{\alpha^2+2}\right)^2, \quad \lambda_4 = 0. \tag{16}$$

and for the nonsymmetric case $\varrho_{12}$

$$\lambda_1 = \left(\frac{(\alpha+1)^2}{\alpha^2+2}\right)^2, \quad \lambda_2 = \left(\frac{(\alpha-1)^2}{\alpha^2+2}\right)^2, \quad \lambda_3 = \lambda_4 = \left(\frac{1}{\alpha^2+2}\right)^2. \tag{17}$$

where $\alpha = (J + \sqrt{8D^2 + J^2})/2D$. It should mention that the above $\lambda_i$s are arranged in descending order in the $D > 0$ region and for $D < 0$ region they will change which we do not show here. In order to determine the existence of entanglement, we have considered ferromagnetic and antiferromagnetic cases. Figures 6 and 7 show symmetric, $C_{13}$, and nonsymmetric, $C_{12}$, concurrences.

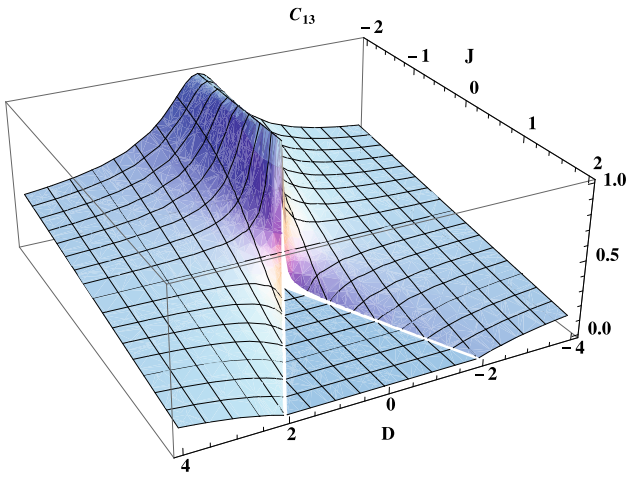


**Fig. 6** (Color online) The ground state entanglement through symmetric way, $C_{13}$, for both antiferromagnetic and ferromagnetic cases as function of DM and $J$ exchange

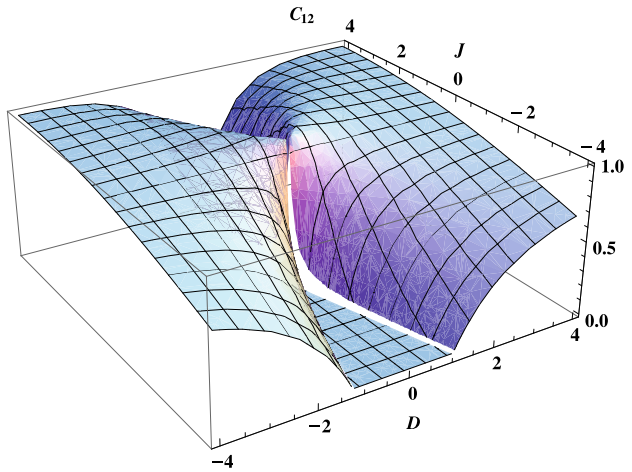


**Fig. 7** (Color online) The ground state entanglement through non-symmetric way, $C_{12}$, for both antiferromagnetic and ferromagnetic cases as function of DM and $J$ exchange

*In the symmetric way*, Fig. 6, it is clear that with the absence of DM interaction the ferromagnetic case is entangled, in contrast to antiferromagnetic case which is fully disentangled. In the antiferromagnetic case, the $C_{13}$ is zero up to critical line $D_c = |J|$ and then after that starts to increase by increasing DM up to a saturation value. In the ferromagnetic case, the system is entangled and by increasing DM interaction it starts to decrease. In both antiferromagnetic and ferromagnetic cases, in the entangled region, there is a competition between Ising exchange $J$ and the DM interaction which has different roles in two cases.

*In the nonsymmetric way*, Fig. 7, ferromagnetic Ising chain with added DM interaction does not show any entanglement behavior up to critical line $D_c = |J|$. But for $D_c > |J|$, entanglement starts to increase by increasing DM interaction. The antiferromagnetic chain is fully entangled. Indeed, $C_{12}$ starts to increase from zero as soon as the DM is turned on and reaches a saturated value around $D_c = |J|$. It should be mentioned that, contrary to ferromagnetic case which increasing $J$ exchange causes to decrease $C_{12}$, in the antiferromagnetic case, increasing Ising exchange coupling $J$ can enhance the amount of entanglement.

In what follows, we will focus on thermal entanglement behavior of three qubits in the two symmetric and nonsymmetric ways. The concept of thermal entanglement was introduced and studied within one-dimensional isotropic Heisenberg model [46, 47]. The state of the system at thermal equilibrium is $\rho(T) = \exp(-H/kT)/\Omega$, where $\Omega = Tr[\exp(-H/kT)]$ is the partition function and $k$ is the Boltzmann's constant. As $\rho(T)$ represents the thermal state, the entanglement in the state is called thermal entanglement [46, 47]. The square roots of the operator $\varrho_{ij}(T)$ for symmetric and nonsymmetric cases are presented in sequence. For the nonsymmetric case $\varrho_{13}(T)$,

$$\lambda_1 = \lambda_2 = X_{12}^2, \quad \lambda_3 = (Y_{12} + Z_{12})^2, \quad \lambda_4 = (Y_{12} - Z_{12})^2 \tag{18}$$

where

$$X_{12} = \frac{1}{\Omega}\left[\frac{1}{2} + \frac{e^{-\beta\varepsilon_3}}{a^2+2} + e^{-\beta\varepsilon_5} + \frac{e^{-\beta\varepsilon_7}}{b^2+2}\right],$$
$$Y_{12} = \frac{1}{\Omega}\left[\frac{1}{2} + \frac{(a^2+1)e^{-\beta\varepsilon_3}}{a^2+2} + \frac{(b^2+1)e^{-\beta\varepsilon_7}}{b^2+2}\right], \tag{19}$$
$$Z_{12} = \frac{1}{\Omega}\left[\frac{2ae^{-\beta\varepsilon_3}}{a^2+2} + \frac{2be^{-\beta\varepsilon_7}}{b^2+2}\right],$$

and for the nonsymmetric case $\varrho_{12}(T)$

$$\lambda_1 = \lambda_2 = X_{13}^2, \quad \lambda_3 = (Y_{13} + Z_{13})^2, \quad \lambda_4 = (Y_{13} - Z_{13})^2 \tag{20}$$

where

$$X_{13} = \frac{1}{\Omega}\left[\frac{a^2e^{-\beta\varepsilon_3}}{a^2+2} + e^{-\beta\varepsilon_5} + \frac{b^2e^{-\beta\varepsilon_7}}{b^2+2}\right],$$
$$Y_{13} = \frac{1}{\Omega}\left[1 + \frac{2e^{-\beta\varepsilon_3}}{a^2+2} + \frac{2e^{-\beta\varepsilon_7}}{b^2+2}\right], \tag{21}$$
$$Z_{13} = \frac{1}{\Omega}\left[1 - \frac{2e^{-\beta\varepsilon_3}}{a^2+2} - \frac{2e^{-\beta\varepsilon_7}}{b^2+2}\right],$$

and $\Omega = 4e^{-\beta J}[\cosh\beta J + \cosh\beta q]$, $a = (J-q)/2D$, $b = (J+q)/2D$, $\varepsilon_1 = \varepsilon_2 = 0$, $\varepsilon_3 = \varepsilon_4 = 2J$, $\varepsilon_5 = \varepsilon_6 = -J+q$, $\varepsilon_7 = \varepsilon_8 = -J-q$, where $q = \sqrt{8D^2+J^2}$. In Fig. 8 and Fig. 9, we give two plots of the thermal concurrence of antiferromagnetic and ferromagnetic Ising chains as functions of temperature and DM interaction respectively.

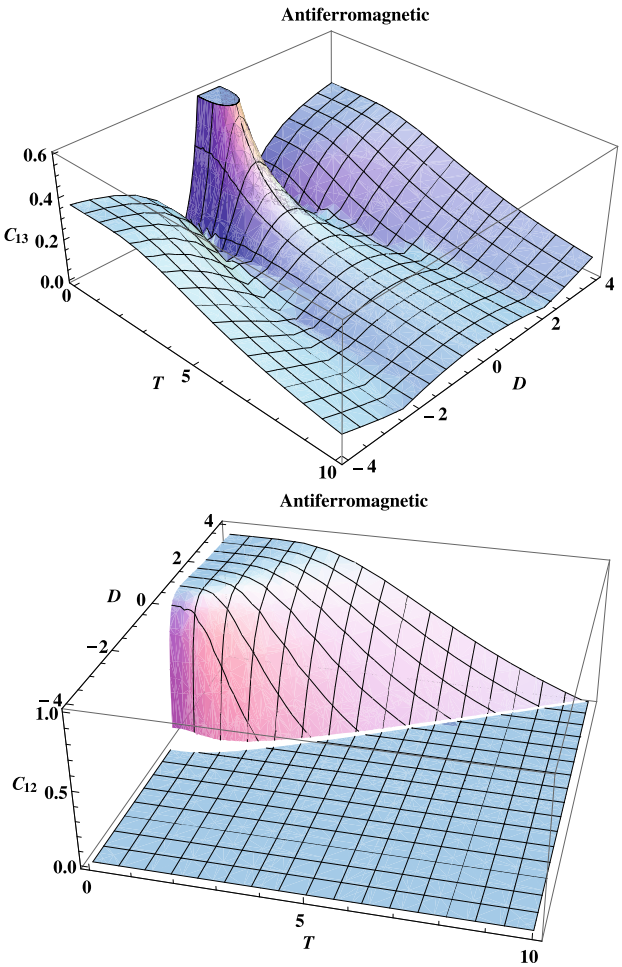


**Fig. 8** The thermal entanglement through symmetric way (*top*), $C_{13}$, and nonsymmetric way (*bottom*), $C_{12}$, for antiferromagnetic case as a function of DM and temperature

*In the antiferromagnetic case*, Fig. 8, with the absence of DM interaction, system is fully entangled through symmetric way. Soon after turning DM interaction, in the low temperature region, $C_{13}(T)$ starts to decrease very fast and reaches zero at a critical line in the $(J–D)$ plane and then after that increasing DM interaction causes to enhance the amount of $C_{13}(T)$ monotonically up to its saturation value. Since no matter what the value of DM is, $C_{13}(T)$ monotonically decreases with the increase of temperature until it reaches the critical value of $T_c$, which depends on the magnitude of DM interaction, and becomes zero. $C_{13}(T)$ also shows symmetric behavior with respect to the DM value. In the nonsymmetric way for antiferromagnetic chain scenario is different. $C_{12}(T)$ is no longer symmetric with respect to the DM value and is zero value for $D < 0$. For $D > 0$, the situation is opposite and $C_{12}(T)$ maintains a maximal value of $C_{12}(T) = 1.0$ until first critical value of $T_{c1}$ and then monotonically decreases with the increase of temperature until it reaches the second critical value of $T_{c2}$, which depends on the magnitude of DM interaction, and becomes zero.

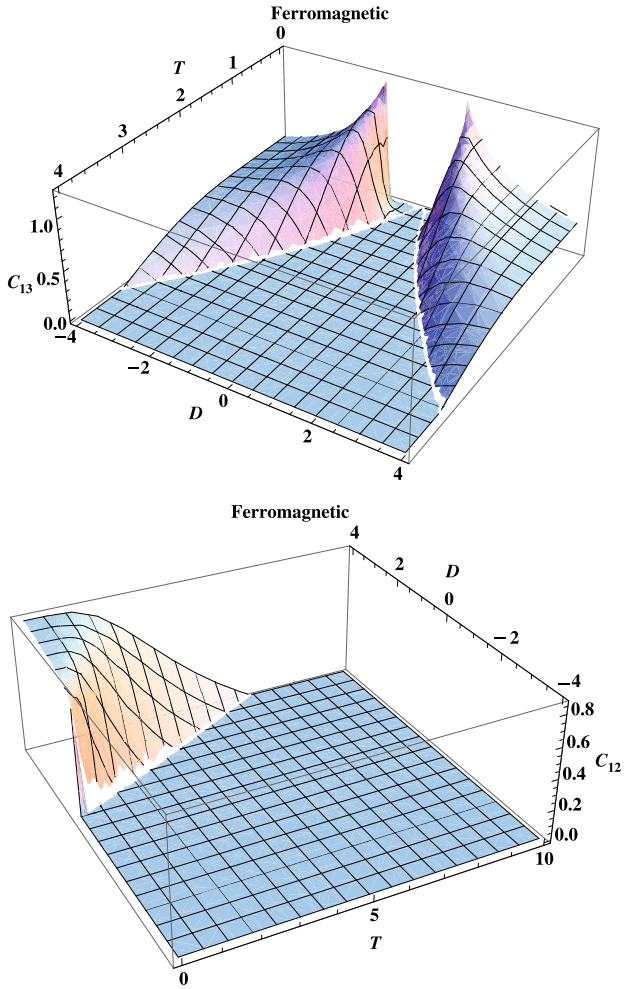


**Fig. 9** The thermal entanglement through symmetric way (*top*), $C_{13}$, and nonsymmetric way (*bottom*), $C_{12}$, for the ferromagnetic case as a function of DM and temperature

*In the ferromagnetic case*, Fig. 9, entanglement through the nonsymmetric way $C_{12}(T)$ behaves qualitatively the same as its antiferromagnetic counterpart, just with different critical temperature points. In the symmetric way, $C_{13}(T)$ is symmetric with respect to the DM value and it is zero up to a critical line in the $(D–T)$ plane. By increasing the DM interaction, $C_{13}(T)$ starts very fast to increase up to a maximal value and then after that monotonically decreases with the increase of DM interaction until it reaches a saturation value.

## 5 Conclusion

To summarize, we have investigated the effect of a Dzyaloshinskii–Moriya (DM) interaction on the ground state phase diagram of the one-dimensional (1D) Ising spin-1/2 model using the variational matrix product state and numerical Lanczos methods from an entanglement point of view. Our results show that there is a critical point in either ferromagnetic and antiferromagnetic cases. In the ferromagnetic Ising chain, this critical point was predicted by variational matrix approach exactly at $D_c = |J|$, which by using numerical study we have confirmed it. We have also used the minimum of the entanglement ratio $R \equiv \tau_2/\tau_1 < 1$, to check the presence of this quantum critical point. For both ferromagnetic and antiferromagnetic cases, our numerical study gave the minimum of $R \equiv \tau_2/\tau_1$ at $D_c = |J|$. We also used generalized multipartite entanglement tools to check how entanglement is used to share in our model and check their ability to detect the critical point. For the antiferromagnetic case, we have calculated global $E_{gl}$ and generalized multipartite entanglement $G(2, n)$ and both of them show that a quantum phase transition took place at $D_c = |J|$ .

We have calculated ground state entanglement of symmetric, $C_{13}$, and nonsymmetric, $C_{12}$, concurrences for ferromagnetic and antiferromagnetic cases. For the symmetric way, with the absence of DM interaction, antiferromagnetic case is fully disentangled. By increasing DM, in the antiferromagnetic case, the $C_{13}$ maintains zero value up to a critical point $D_c = |J|$. After the critical point entanglement starts to increase until a saturation value. For ferromagnetic case, in the symmetric way, $C_{13}$ is always different from zero and it decreases by increasing DM interaction. In the nonsymmetric way, with the absence of DM interaction, $C_{12}$ is equal zero for both antiferromagnetic and ferromagnetic cases. By turning DM, in the ferromagnetic case, nothing happens up to a critical point $D_c$ and then after that $C_{12}$ starts to increase by increasing DM interaction. In contrast to ferromagnetic case, in the antiferromagnetic case, $C_{12}$ starts to increase immediately after turning DM interaction and reaches a saturation value around $D_c = |J|$.

We have also studied thermal entanglement of symmetric, $C_{13}(T)$, and nonsymmetric, $C_{12}(T)$ for both ferromagnetic and antiferromagnetic cases. Our calculations show that for either symmetric and nonsymmetric cases thermal (disentanglement favorable) and quantum (entanglement favorable) fluctuations have competition to drive the system to their favorable regime.

**Acknowledgements** It is our pleasure to thank S. Montangero, R. Jafari, and E. Mehran for their very useful comments.

## References

1. Nielsen, M.A., Chuang, I.L.: Quantum Computation and Quantum Information. Cambridge University Press, Cambridge (2000)
2. Wang, X.: Phys. Rev. A **64**, 012313 (2001)
3. Arnesen, M.C., Bose, S., Vedral, V.: Phys. Rev. Lett. **87**, 017901 (2001)
4. Osborne, T.J., Nielsen, M.A.: Phys. Rev. A **66**, 032110 (2002)
5. Osterloh, A., Amico, L., Falci, G., Fazio, R.: Nature **416**, 608 (2002)

6. Vidal, G., Latorre, J.I., Rico, E., Kitaev, A.: Phys. Rev. Lett. **90**, 227902 (2003)
7. Wu, L.A., Sarandy, M.S., Lidar, D.A.: Phys. Rev. Lett. **93**, 250404 (2004)
8. Dur, W., Hartmann, L., Hein, M., Lewenstein, M., Briegel, H.J.: Phys. Rev. Lett. **94**, 097203 (2005)
9. Guhne O, O., Toth, G., Briegel, H.J.: New J. Phys. **7**, 229 (2005)
10. Lou, P., Lee, J.Y.: Phys. Rev. B **74**, 134402 (2006)
11. Amico, L., Fazio, R., Osterloh, A., Vedal, V.: Rev. Mod. Phys. **80**, 517 (2008)
12. Horodecki, R., Horodecki, P., Horodecki, M., Horodecki, K.: Rev. Mod. Phys. **81**, 865 (2009)
13. Sachdev, S.: Quantum Phase Transitions. Cambridge University Press, Cambridge (2000)
14. Osterloh, A., et al.: Nature (London) **416**, 608 (2002)
15. Wooters, W.K.: Phys. Rev. Lett. **80**, 2245 (1998)
16. Vidal, G., Werner, R.F.: Phys. Rev. A **65**, 032314 (2002)
17. Dzyaloshinskii, I.: J. Phys. Chem. Solids **4**, 241 (1958)
18. Moriya, T.: Phys. Rev. Lett. **4**, 228 (1960)
19. Perk, J.H.H., Capel, H.W.: Phys. Lett. A **58**, 115 (1976)
20. Kadar, Z., Zimboras, Z.: Phys. Rev. A **82**, 032334 (2010)
21. Sudan, J., Luscher, A., Lauchli, A.M.: Phys. Rev. B **80**, 140402(R) (2009)
22. Seki, S., Yamasaki, Y., Soda, M., Matsuura, M., Hirota, K., Tokura, Y.: Phys. Rev. Lett. **100**, 127201 (2008)
23. Huvonen, D., Nagel, U., Room, T., Choi, Y.J., Zhang, C.L., Park, S., Cheong, S.W.: Phys. Rev. B **80**, 100402(R) (2009)
24. Oshikawa, M., Affleck, I.: Phys. Rev. Lett. **82**, 5136 (1999)
25. Affleck, I., Oshikawa, M.: Phys. Rev. B **60**, 1038 (1999)
26. Derzhko, O., Verkholyak, T., Krokhmalskii, T., Buttner, H.: Phys. Rev. B **73**, 214407 (2006)
27. Kargarian, M., Jafari, R., Langari, A.: Phys. Rev. A **79**, 042319 (2009)
28. Garate, I., Affleck, I.: Phys. Rev. B **81**, 144419 (2010)
29. Soltani, M.R., Mahdavifar, S., Akbari, A., Masoudi, A.A.: J. Supercond. Nov. Magn. **23**, 1369 (2010)
30. Jafari, R., Kargarian, M., Langari, A., Siahatgar, M.: Phys. Rev. B **81**, 054413 (2008)
31. Roscilde, T., Verrucchi, P., Fubini, A., Haas, S., Tognetti, V.: Phys. Rev. Lett. **93**, 167203 (2004)
32. Roscilde, T., Verrucchi, P., Fubini, A., Haas, S., Tognetti, V.: Phys. Rev. Lett. **94**, 147208 (2005)
33. Bennett, C.H., DiVincenzo, D.P., Smolin, J.A., Wootters, W.K.: Phys. Lett. A **54**, 3824 (1996)
34. Amico, L., Osterloh, A., Plastina, F., Fazio, R., M Palma, G.: Phys. Lett. A **69**, 022304 (2004)
35. Coffman, V., Kundu, J., Wootters, W.K.: Phys. Rev. A **61**, 052306 (2000)
36. Osborne, T.J., Verstraete, F.: Phys. Rev. Lett. **96**, 220503 (2006)
37. Meyer, D.A., Wallach, N.R.: J. Math. Phys. **43**, 4273 (2002)
38. Montakhab, A., Asadian, A.: Phys. Rev. A **82**, 062313 (2010)
39. de Oliveira, T.R., Rigolin, G., de Oliveira, M.C.: Phys. Rev. A **73**, 010305(R) (2006)
40. Rigolin, G., de Oliveira, T.R., de Oliveira, M.C.: Phys. Rev. A **74**, 022314 (2006)
41. de Oliveira, T.R., Rigolin, G., de Oliveira, M.C., Miranda, E.: Phys. Rev. Lett. **97**, 170401 (2006)
42. Klumper, A., Schadschneider, A., Zittartz, J.: J. Phys. A **24**, L955 (1991)
43. Klumper, A., Schadschneider, A., Zittartz, J.: Z. Phys. B **87**, 281 (1992)
44. Klumper, A., Schadschneider, A., Zittartz, J.: Europhys. Lett. **24**, 293 (1993)
45. Fannes, M., Nachtergaele, B., Werner, R.F.: Europhys. Lett. **10**, 633 (1989)
46. Arnesen, M.C., Bose, S., Verdal, V.: Phys. Rev. Lett. **87**, 017901 (2001)
47. Nielsen, M.A.: Ph.D. Dissertation, The University of New Mexico (1998)